Synthetic Metals 206 (2015) 131–144

Contents lists available at ScienceDirect

Synthetic Metals

journal homepage: www.elsevier.com/locate/synmet

An impressive emulsion polymerization route for the synthesis of highly soluble and conducting polyaniline salts

Salma Bilal [a], Salma Gul [a], Rudolf Holze [b], Anwar-ul-Haq Ali Shah [c,*]

[a] National Centre of Excellence in Physical Chemistry, University of Peshawar, 25120 Peshawar, Pakistan
[b] Institute für Chemie, AG Elektrochemie, Technische Universität Chemnitz, 09107 Chemnitz, Germany
[c] Institute of Chemical Sciences, University of Peshawar, 25120 Peshawar, Pakistan

ARTICLE INFO

Article history:
Received 10 September 2014
Received in revised form 30 April 2015
Accepted 12 May 2015
Available online 2 June 2015

Keywords:
Polyaniline
Chemical synthesis
Electrical conductivity
Thermal properties
Corrosion

ABSTRACT

We report a sophisticated emulsion polymerization route for the synthesis of polyaniline (PANI) salts. In this process, the chemical oxidative polymerization of aniline was carried out in the presence of two dopants i.e., dodecylbenzenesulfonic acid (DBSA) and sulfuric acid (H_2SO_4). The synthesized PANI salts were highly soluble in a large number and variety of common organic solvents (so far highest number of solvents including the less hazardous ethanol) and showed very good conductance. Presumably the presence of DBSA and sulfuric acid moieties, respectively, contributed toward the improvement in solubility and conductance. After optimization of the reaction parameters, the obtained polymers were systematically characterized with cyclic voltammetry, in situ conductance, in situ UV–vis spectroelectrochemical and intrinsic viscosity measurements. X-ray diffraction, TGA and SEM were used for further analysis. The materials showed very good electrochemical and electrochromic reversibility and high thermal stability (up to 500 °C). Moreover, potentiodynamic measurements revealed that coatings of this polymer can provide extra ordinary resistance to the steel surfaces particularly against the harsh corrosive environment of the oceans.

1. Introduction

Polyaniline and its derivatives are the subject of considerable research interest around the globe. The versatile technological applications of this fascinating material in various fields are broadly associated with its good conducting properties. Depending upon the mode of synthesis, nature and concentration of dopants and supporting electrolyte, PANI is collected in different states; leucoemeraldine, emeraldine base, emeraldine salt or pernigraniline. Emeraldine salt is the most promising and the only electrically conducting form of PANI [1].

Although, PANI is a promising candidate for various technological applications such as corrosion protections of metals, rechargeable batteries, capacitors, actuator and sensors [2], it has the drawback of poor processability and solubility in commonly used organic solvents. This limits the applications of PANI to a greater extent. Literature reveal that the properties of PANI greatly depend upon the method of synthesis, types of dopants, oxidants and the solvent system used during its synthesis. For instance, the processability of PANI was reported to be improved significantly by grafting copolymerization of aniline onto a modified surfactant [3]. Considerable progress has been made by the preparation of polymer blends and composites [2]. The solubility of PANI was also reported to be improved considerably by adopting chemical oxidative polymerization routes for the synthesis of substituted PANIs or copolymerization of aniline with substituted anilines and synthesis of PANI by emulsion/inverse emulsion polymerization techniques [4]. In emulsion/inverse emulsion polymerization pathways, different types of surfactants are employed. These surfactants are believed to help in improvement of solubility. At the same time they also act as dopants.

Dodecylbenzenesulfonic acid (DBSA) has emerged as a promising dopant and surfactant and is frequently applied in different protocols for the synthesis of soluble PANI. Some examples are polymerization in solution [5], emulsion/inverse emulsion polymerization [6] and re-doping of emeraldine base (EB-PANI) [7]. The solubility of PANI, doped with dodecylbenzenesulfonic acid (DBSA) or camphor sulfonic acid, in chloroform and xylene has been reported [8]. Yu et al. [9] fabricated a honeycomb-structured film of PANI–DBSA, which was electroactive and semi-conducting in the appropriately doped state. Han et al. [10] reported the synthesis of PANI nanoparticles using DBSA in aqueous DBSA micellar solution. Earlier a new inverse emulsion polymerization

* Corresponding author. Tel.: +92 91 9216652, 9216701-20; fax: +92 91 9216652.
E-mail address: anwarulhaqalishah@upesh.edu.pk (A.-u.-H.A. Shah).

http://dx.doi.org/10.1016/j.synthmet.2015.05.015
0379-6779/

pathway was reported for the synthesis of PANI doped with DBSA using benzoyl peroxide as the oxidizing agent [11]. It was reported that the synthesized PANI was soluble in chloroform but did not show any electrical conductance in aqueous acidic media.

These reports demonstrate that the efforts for enhancing the solubility of PANI in commonly used solvents via different approaches always result in the reduction in the conductance of PANI to different levels [4,12].

Reports are also available on several chemical oxidative polymerization routes adopted for the synthesis of PANI having good conductance. But the results are not impressive. Stejskal et al. [13] studied the effect of various acids on the conductance of PANI. They observed that among various acids such as sulfuric acid, hydrochloric acid, sulfonic acid and carboxylic acid, only hydrochloric acid and sulfuric acid appreciably enhance the conductance of PANI. Borole et al. [14] compared the effect of and Cl^- anions on the conductance of PANI. They found highest conductance for sulfate-doped PANI. However, they did not achieve appreciable solubility. Rao et al. [15] used benzoyl peroxide as a novel oxidizing agent for the synthesis of PANI. The PANI salts synthesized by this pathway showed good conductance but low solubility.

Here we report an emulsion polymerization pathway for the synthesis of PANI. The beauty of the route arises from the fact that the synthesized PANI salts were found to be highly soluble and conducting. To the best of our knowledge there is no report on the synthesis of PANI, neither via electrochemical polymerization nor via chemical oxidative polymerization, where the synthesized PANI is highly soluble in a large number of common organic solvents and at the same time exhibits good conductance. In this process dodecylbenzenesulfonic acid (DBSA) and sulfuric acid, were both used together as dopants, resulting in the formation PANI–DBSA–H_2SO_4. The long alkyl chain of DBSA is supposed to impart solubility to the synthesized polymer in common organic solvents. The sulfate moiety can provide a good conductive structure because it may cause less hindrance as compared to bulky alkyl group of DBSA. The synthesized PANI–DBSA–H_2SO_4 salts seem to deserve their application in various technologies such as corrosion protection of metals.

2. Experimental

2.1. Materials and chemicals

All chemicals were of analytical grade. Aniline (Riedel-de Häen) was distilled under reduced pressure and stored under nitrogen in a refrigerator. H_2SO_4 (Riedel-de Häen), chloroform (Scharlau), DBSA (Aldrich), ammonium persulfate, APS (Riedel-de Häen) were used as received, Ultrapure water (Millipore) was used for solution preparation and natural water of Indian and Pacific Oceans was used for corrosion tests.

2.2. Synthesis of polyaniline

In a typical experiment, 7.47 mmol of DBSA was slowly added to 50 mL of chloroform under constant stirring. Then 16.42 mmol of aniline was added to this mixture. It was followed by the drop wise addition of 25 mL of an aqueous solution of sulfuric acid (12.50 mmol) and 25 mL of an aqueous solution of the oxidant, APS, (1.25 mmol). Consequently the formation of a milky white emulsion was observed. The stirring was continued at room temperature. The content of the round-bottom flask gradually turned green. After about 24 h, the mixture was transferred in to a separating flask and kept for 15 min to separate the organic and aqueous phases. Afterwards, the organic phase was washed repeatedly with deionized water and added to 50 mL of acetone in order to precipitate out the polymer. The obtained green precipitate was filtered under suction and washed with excess of acetone. It was then kept overnight in an oven at 60 °C for drying.

By following the above mentioned procedure, the amounts of reactants (i.e., sulfuric acid, aniline and APS) were stepwise changed in the feed for optimization. Details of the synthesized samples are listed in Table 1.

2.3. Characterization

Percent yield of PANI was calculated by using the following formula:

$$\text{Percentyield} = \frac{\text{Weightofpolyaniline}}{\text{Weightofaniline}} \times 100 \quad \text{(i)}$$

As basically we wanted to observe the effect of the amount of the H_2SO_4 on the properties of the resulting polyaniline salts, seven samples (sample numbers 1–7 in Table 1) were synthesized with varying amounts of H_2SO_4. Of these samples, sample number 1 (with 3.75 mmol of H_2SO_4) sample number 4 (with 12.5 mmol of H_2SO_4) and sample number 7 (with 25.00 mmol of H_2SO_4) were selected for further studies. The amounts of aniline, APS and DBSA were kept constant as 16.42 mmol, 1.25 mmol and 7.47 mmol, respectively. For the sake of convenience and clarity, samples number 1, 4 and 7 were further labeled as PANI 1, PANI 2 and PANI 3, respectively. These samples demonstrate the lowest, intermediate and highest amounts of the acid in presently studied range, while keeping all the other parameters constant.

The following procedure was adopted for the determination of maximum attainable concentration of the synthesized materials in a particular solvent (e.g., in chloroform). For this purpose 10 mL of chloroform was taken and 1 g of the sample was gradually added to it. When some of the polymer did not dissolve, further 3 mL of chloroform was added to dissolve it. The solubility was then calculated in percent weight/volume (w/v%). In this way, the solubility of the synthesized materials was determined in a variety of organic solvents as demonstrated in Fig. 2.

Cyclic voltammetry was performed by means of 3000 ZRA potentiostat/galvanostat Gamry (USA). Cyclic voltammograms were recorded in a three electrode cell containing 0.5 M H_2SO. PANI dissolved in ethanol was dip-coated onto a gold sheet and it was used as working electrode. A gold coil and a saturated calomel

Table 1
Composition of various samples of PANI–DBSA–H_2SO_4 salts. Samples 1–7 were synthesized with varying amounts of H_2SO_4. Samples 8–13 were synthesized with varying amounts of aniline while in samples 14–19 the amount of APS was changed.

S. No	H_2SO_4 (mmol)	Aniline (mmol)	APS (mmol)
1	3.75	16.42	1.25
2	5.00	16.42	1.25
3	7.50	16.42	1.25
4	12.50	16.42	1.25
5	17.50	16.42	1.25
6	22.50	16.42	1.25
7	25.00	16.42	1.25
8	12.50	1.09	1.25
9	12.50	5.47	1.25
10	12.50	10.95	1.25
11	12.50	16.42	1.25
12	12.50	21.90	1.25
13	12.50	27.38	1.25
14	12.50	16.42	0.25
15	12.50	16.42	0.50
16	12.50	16.42	0.75
17	12.50	16.42	1.00
18	12.50	16.42	1.50
19	12.50	16.42	1.75

electrode (SCE) served as the counter and reference electrodes, respectively.

UV–vis spectra of PANI solution in ethanol were recorded with a PerkinElmer 650 (UK) spectrophotometer. In situ UV–vis spectroelectrochemical studies were carried out in a spectroelectrochemical cell containing an optically transparent ITO coated glass as working electrode. A platinum wire and SCE were used, respectively, as counter and reference electrode. Before each experiment, the ITO coated glass sheets were degreased with acetone and rinsed with plenty of ultrapure water. Before each spectroscopic measurement baseline correction was made with ITO glass electrodes placed in both instrument channels containing 0.5 M H_2SO_4 solution. The reference electrode was connected to the cuvette with a salt bridge. In the reference channel of the spectrometer an ITO coated glass electrode without polymer coating was inserted in a quartz cuvette. UV–vis spectra were collected continuously at different applied potentials for the respective polymer films, with a PC-driven Shimadzu UV-2101 PC scanning spectrometer (resolution 0.1 nm, spectra recording time 1 min).

FTIR spectra of PANIs, in KBr pellets, were recorded in the range 400–4000 cm^{-1} by means of Shimadzu (Japan) spectrometer.

For the study of in situ conductance, the polymer film was drop-coated on a double-band gold electrode and the resistance at different applied potentials was measured with a specially designed electronic circuit described elsewhere [16]. A gold sheet was used as counter electrode while saturated calomel electrode was employed as reference electrode. The measurements were carried out in aqueous H_2SO_4 in a three electrode cell. Electrode potential was increased stepwise by 50 mV. The film resistance (R_x) was calculated from the measured voltage (U_x) and amplification factor (F_{ac}) by using the following relation:

$$R_x = \frac{0.01 \times F_{ac}}{U_x} \quad \text{(ii)}$$

The X-ray diffraction patterns of PANI samples were recorded at room temperature in the range 1–70° with a continuous scan speed of 0.05°/s by means of a Rigaku X-Ray diffractometer (Japan) having copper Kα radiation with a wavelength of 1.5405 Å. Thermal analysis of the synthesized samples was carried out in N_2 atmosphere by using a PerkinElmer thermogravimetric analyzer (USA) at a heating rate of 10 °C/min.

Viscosities of PANI–DBSA–H_2SO_4 were determined with the help of a capillary viscometer. Experiments were carried out at five gradually diluted concentrations (0.005, 0.004, 0.003, 0.002 and 0.001 g/mL) using ethanol as a solvent. Intrinsic viscosity (η) was obtained by linear extrapolation of the line of specific viscosity divided by the concentration (η_{sp}/c) vs. concentration (c) and the line of the natural logarithm of relative viscosity divided by concentration ($\ln \eta_{rel}/c$) vs. concentration (c) to the same intercept at zero concentration [17].

Morphological features and size of the particles were analyzed with a scanning electron microscope [JSM-5910, JEOL]. In every case, the sample was made by mounting a little amount of the given powder on an aluminum stub using double-coated conducting carbon adhesive tape. Samples were coated with gold using auto fine coater [JEOL, JFC-1600] for the duration of 30 s. The working distance was kept 10 mm from the sample to electron gun tip and the accelerating voltage was adjusted to 15 kV.

2.4. Corrosion test

The corrosion protection performance of PANI–DBSA–H_2SO_4 salt was studied in natural water of the Indian and Pacific Oceans. The experiments were performed in a single compartment 3-electrode cell. Steel discs (stainless steel and mild steel) were used as working electrodes. Saturated calomel electrode (SCE) and gold electrodes were used as reference and counter electrodes, respectively. Before coating with the polymer, steel was polished with abrasive paper and rinsed with mixture of acetone and ethanol and finally with distilled water. The polymer dissolved in ethanol, was drop coated on to the steel electrode. Potentiodynamic polarization measurements were performed by scanning the potential from −250 mV to +250 mV and vice versa (cathodic/anodic plots).

The potentiodynamic current density–potential curve (Tafel plot) was recorded by means of 3000 ZRA potentiostat/galvanostat Gamry (USA) with DC105 DC Corrosion Techniques Software running on a personal computer. The obtained data was analyzed by Gamry Echem Analyst software in order to extract the values of corrosion potential (E_{cor}), corrosion current (i_{cor}) and corrosion rate (CR mm/year) of steel electrodes. The software established Tafel slopes for anodic and cathodic reactions and extrapolated back to the point where the anodic and cathodic reaction rates (i.e., currents) were equivalent. The current density at that point was noted as the corrosion current density (i_{cor}) and the potential at which it falls was recorded as the corrosion potential (E_{cor}).

3. Results and discussion

3.1. Effect of reaction parameters on yield

PANI–DBSA–H_2SO_4, were prepared by emulsion polymerization of aniline using ammonium persulfate as an oxidant. The reaction parameters were optimized systematically by varying the amounts of oxidant, monomer and acid, respectively, in the feed. Fig. 1a

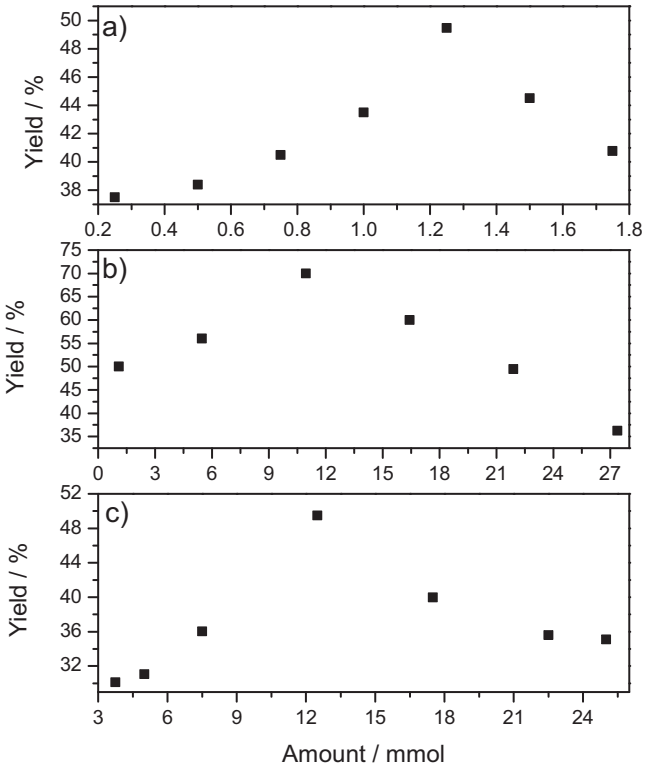

Fig. 1. The influence of synthesis parameters on the percent yield of PANI–DBSA–H_2SO_4 salts. (a) amount of oxidant at constant amount of aniline (16.42 mmol), DBSA (7.47 mmol) and H_2SO_4 (12.5 mmol); (b) amount of aniline at constant amount of the oxidant (1.25 mmol), DBSA (7.47 mmol) and H_2SO_4 (12.5 mmol); (c) amount of H_2SO_4 at constant amount of aniline (16.42 mmol), DBSA (7.47 mmol) and oxidant (1.25 mmol).

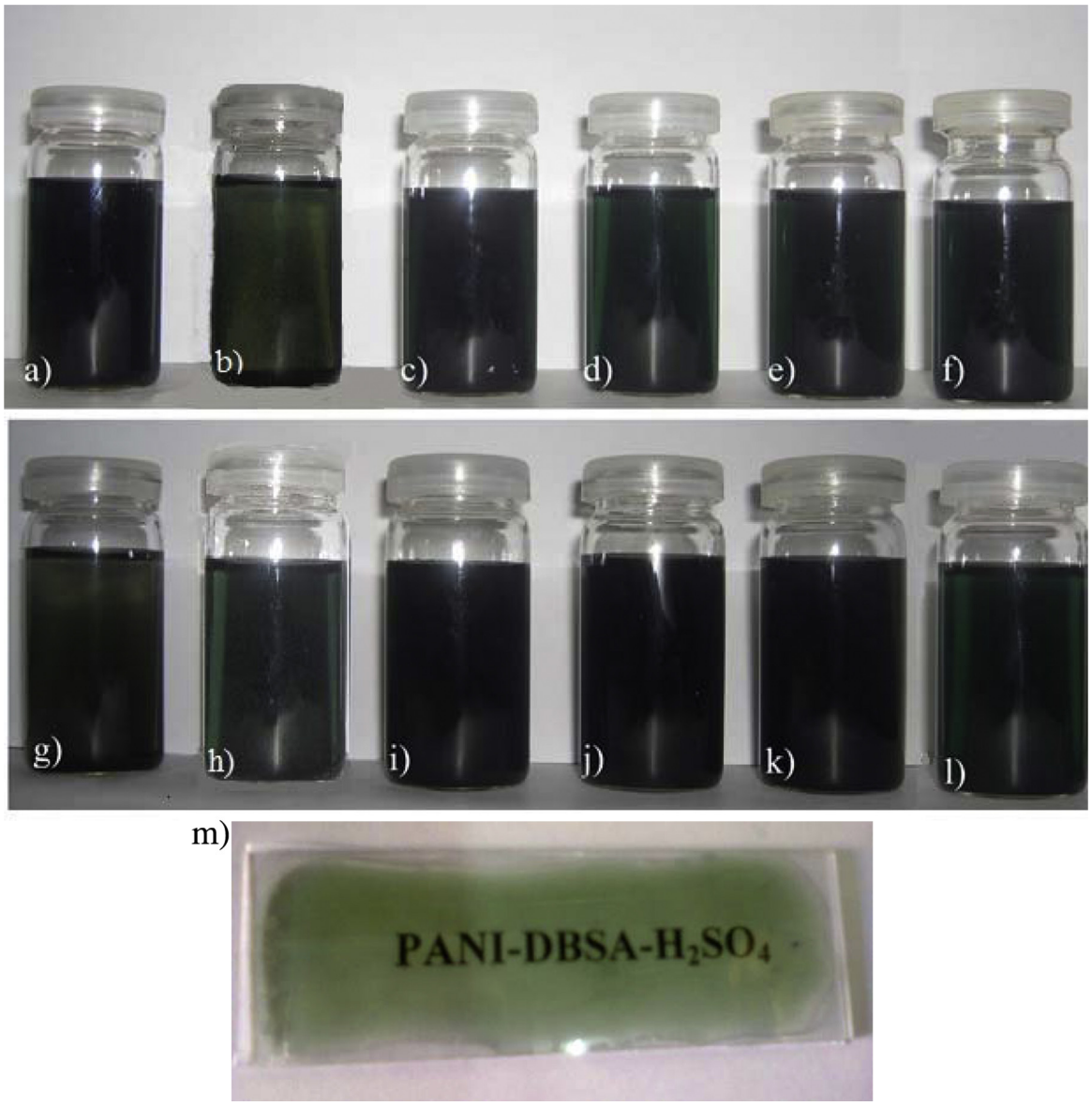

Fig. 2. Solutions of PANI–DBSA–H_2SO_4 in (a) tetrahydrofuran, 9.1% w/v, (b) m-cresol, 7% w/v, (c) dimethylsulfoxide, 8.2% w/v, (d) *N*-methyl-2-pyrrolidone, 8.2% w/v, (e) dimethylformamide, 8% w/v, (f) 2-propanol, 6.5% w/v, (g) ethanol, 6.5% w/v, (h) chloroform, 7.6% w/v, (i) 1,2-dichloroethane, 7.1% w/v, and (j) mixture of toluene and 2-propanol, 8.6% w/v, (k) xylene, 5%w/v, (l) toluene, 4.5% w/v. (The values show maximum attainable concentration of PANI 1 in the respective solvent), (m) glass substrate coated with PANI 1 film.

shows the effect of oxidant amount on the yield of PANI–DBSA–H_2SO_4.

It is evident from Fig. 1(a) that the yield of the product increases with the increase in the amount of the oxidant in the range of 0.25 to 1.25 mmol. Further increase in the amount of the oxidant shows a retarding effect on the polymer yield. This can be attributed to the overoxidation of radical cations responsible for both the decrease in growth rate and the chain length of polymer. However, low polymer yield at lower concentration of the oxidant might be due to the decrease in concentration of radical cations [18]. Fig. 1(b) demonstrates that polymer yield increases progressively with the amount of aniline and the yield is maximum at 10.95 mmol in the presently studied range. The initial increase in the percent yield is quite expected. However, the drop in the yield beyond 10.95 mmol may be envisaged as due to the lowering in oxidant's efficiency to oxidize relatively greater amount of monomers with constant initiator amount [19].

Fig. 1(c) depicts the role of amount of acid on the polymer yield. The yield increases with the increase in the amount of acid from 3.75 to 12.5 mmol but decreases with further increase. Ayad and Sheneshin [20] have observed such trend during the synthesis of polyaniline. They suggested that with the increase in acid amount, the electrostatic repulsion inside PANI chain and between similarly charged units of the chain increases. It promotes the extended conformation of chain and thus the yield increases [20]. At higher amount of acid, the PANI chain undergoes hydrolysis causing the yield of PANI salts to decrease [21].

3.2. Solubility

After successful synthesis of PANI–DBSA–H_2SO_4, the solubility of these materials was tested and determined in various organic solvents. These include the commonly used polar solvents such as tetrahydrofuran (THF), m-cresol, dimethyl sulfoxide (DMSO), *N*-

methyl-2-pyrrolidone (NMP), dimethylformamide (DMF), 2-propanol, ethanol and non polar solvents like chloroform, 1,2-dichloroethane, xylene, toluene. Chemical nature of all these organic solvent is quite different from one another. It is a matter of fact that the solubility of PANI can be affected by the interactions among PANI chains, the associated counter ions and the solvent. Therefore, differences in the values of maximum attainable concentration of PANI–DBSA–H_2SO_4 in the mentioned organic solvents were expected. Fig. 2 exemplifies the saturated solutions of PANI 1, along with maximum attainable concentrations of the polymer, in the organic solvents used in this study. The PANI–DBSA–H_2SO_4 readily dissolved in the polar solvents. Perhaps the polar organic solvents enable an effective interaction with PANI chains through protonation or the formation of H—bonds with amine or imine nitrogen [22]. It was revealed previously that such kind of rapid dissolution of PANI in the polar organic solvent will only be possible if a good PANI-acid molar ratio exist in the synthesized sample [22]. Therefore, it can be assumed that the easy dissolution of PANI–DBSA–H_2SO_4 in the polar organic solvents, in the present study, is a result of the fine protonation of the synthesized PANI sample.

As presented in Fig. 2, PANI–DBSA–H_2SO_4 also showed appreciable solubility in non polar organic solvents such as 1,2-dichloroethane, toluene and xylene. In this case, the negative charged sulfonate group of DBSA is expected to interact with the positively charged backbone of the PANI through coulombic attraction and provides a hydrophobic side chain (dodecyl group) for compatibility with non-polar organic solvents. The dopant molecules present in the PANI chains may provide space for penetration of solvent molecules inside the chain and induces its solubility in non polar solvents [23].

However, chloroform showed different behavior for dissolution of PANI–DBSA–H_2SO_4. Unlike above mentioned non polar solvents, the synthesized salts readily dissolved in it. The reason may lies in the fact that in chloroform ($CHCl_3$), the carbon atom is bound to one hydrogen atom and three electronegative atoms (Cl). Due to the difference in the electronegativities of the atoms, the hydrogen atom is believed to form hydrogen bond with PANI, like other polar solvent, and thus enhances its solubility in chloroform.

The solubility of PANI–DBSA–H_2SO_4 was also tested a mixture of two solvents containing a polar solvent (for example 2-propanol) and a non polar solvent (such as toluene). The maximum attainable solubility of the synthesized PANI was higher than the one obtained for 2-propanol and toluene alone (Fig. 2). This can be explained on the bases of complementary effects of the two solvents. 2-propanol has two kinds of groups i.e., a polar (OH) group and a non-polar (alkyl) group. When it is mixed with toluene (a non-polar solvent), the non-polar part of 2-propanol can readily interacts with toluene and form a sizeable non-polar group [22]. Such mixture of solvents can be expected to communicate in two fashions with PANI–DBSA–H_2SO_4. Its polar part forms H-bond with the protonated PANI whereas its fairly large non-polar part easily interacts with the non-polar alkyl chain of DBSA [22].

Thus, these interactions may lead to the enhancement of solubility of the polymer. These observations are important because the properties of a casted film of PANI from a solution are determined by the interactions between the PANI chains, the associated counterion and type of solvent. And so these interactions can easily be tuned by selecting appropriate types of solvents. The synthesized PANI–DBSA–H_2SO_4 can effectively be coated on a metallic or glass substrate. For instance, PANI film coated on a glass substrate is given in Fig. 2 (m). The clear visibility of the text (PANI–DBSA–H_2SO_4) behind the film confirms the good quality and transparency of the material.

3.3. Cyclic voltammetry

Electrochemical behavior of the synthesized PANI–DBSA–H_2SO_4 was investigated with cyclic voltammetry. Cyclic voltammograms (CVs) were recorded by cycling the potential between E_{SCE} − 0.20 and 0.9 V at a scan rate of 50 mV/s (Fig. 3). The products, prepared with different amounts of acid (H_2SO_4) in the

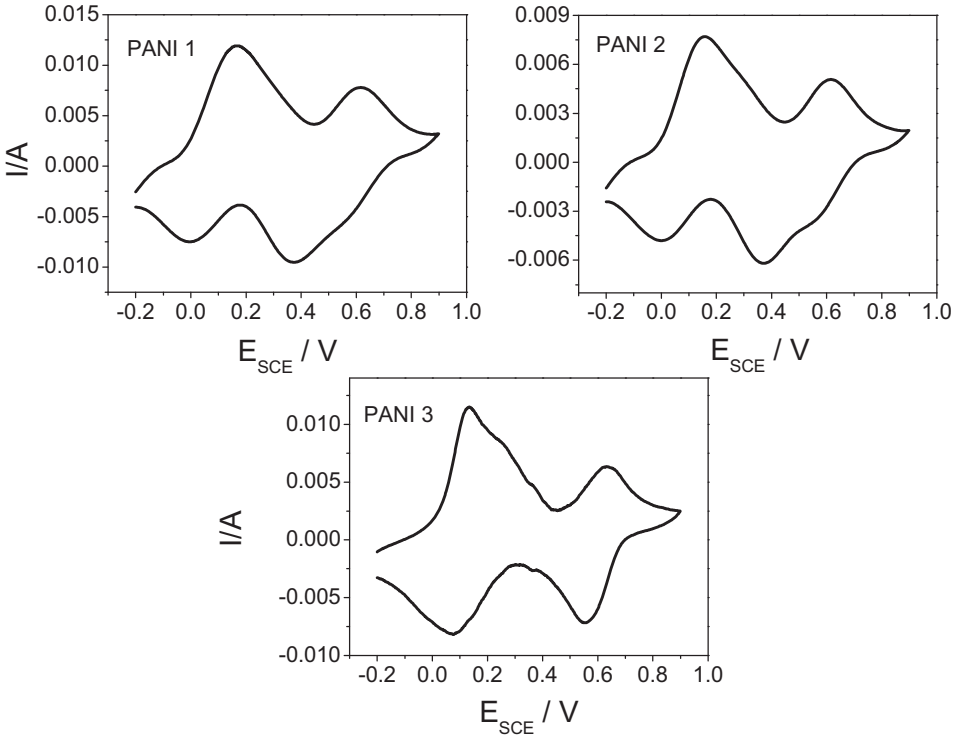

Fig. 3. CVs of PANI–DBSA–H_2SO_4 salts, dip coated on a gold sheet electrode, in 0.5 M H_2SO_4 at a scan rate of 50 mV/s.

polymerization bath, appeared to show very consistent electrochemical behavior.

All the samples show two redox pairs. The first oxidation peak around E_{SCE} = 0.15 V corresponds to the conversion of leucoemeraldine to emeraldine and the second peak around E_{SCE} = 0.60 V corresponds to further transformation of emeraldine into pernigraniline. Mostly a third redox pair, in between the above mentioned redox pairs, is reported to observe in the CV of chemically or electrochemically synthesized PANI [11]. This pair is believed to be associated with the presence of hydrolysis/degradation or overoxidation products incorporated in the polymer chain during the process of synthesis. Such a redox pair is missing in the CVs in Fig. 3. This indicates that the synthesized PANI salts were collected in a very pure form.

CVs of PANI 1 were recorded in the potential range of E_{SCE} − 0.20 to 0.90 V at various scan rates ranging from 0.01 to 0.10 V/s and are displayed in Fig. 4(a). The shape reveals that the polymer exhibits good electroactivity. The redox peak current increases with the scan rate whereas peak potentials remain constant. Generally, the electrode processes are either diffusion or kinetically controlled. In the present study the currents of first anodic peaks are proportional to the square root of scan rate (Fig. 4(b)) which indicates that the electrochemical processes at the polymer-coated electrode surface is diffusion-controlled [24]. At all these scan rates the polymer seems to be quite stable and shows no signs of degradation.

3.4. In situ conductance measurements

Resistance values of PANI–DBSA–H_2SO_4 salts were measured in anodic and cathodic sweeps in the potential range of E_{SCE} = − 0.2 to 0.8 V. The plots of resistance (log R_x) vs. applied potential for PANI 1 and PANI 2 are displayed in Fig. 5. It shows that as the applied potential increases, log R_x remains unchanged up to E_{SCE} = 0.1 V until the offset of first oxidation peak in CV (inset) appears at potential around E_{SCE} = 0.15 V, where log R_x values starts to decrease. Further increase in the potential causes a sharp decrease in resistance until the offset of 2nd oxidation peak in the CV is reached at potential around E_{SCE} = 0.6 V, where resistance begins to increase again. Thus PANI-–DBSA–H_2SO_4 is conductive in the potential range of E_{SCE} = 0.15 to 0.6 V. When the potential sweep direction is reversed from E_{SCE} = 0.8 to − 0.2 V, an almost identical behavior can be observed. However, the minimum resistance during the cathodic sweep is higher than in the anodic sweep [25].

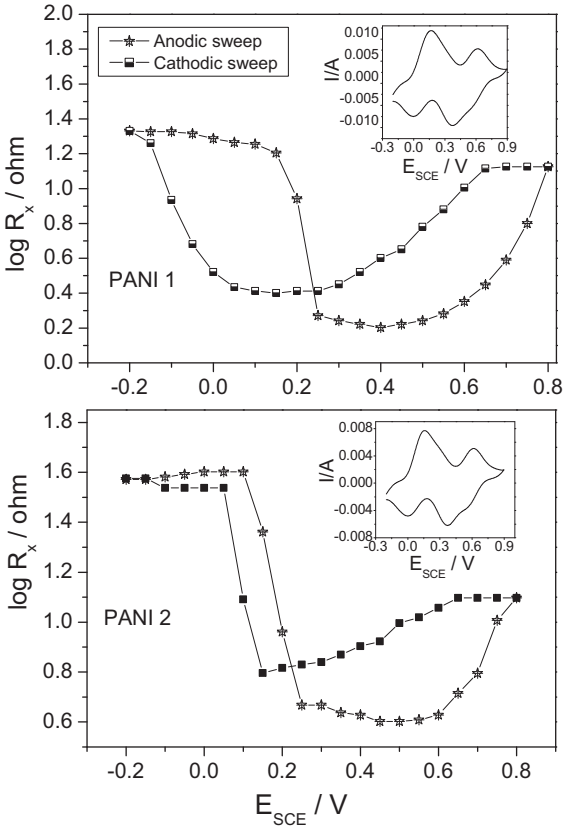

Fig. 5. Plots of resistance vs. applied electrode potential for PANI–DBSA–H_2SO_4 salts. Insets: CV of the corresponding film in 0.5 M H_2SO_4 at a scan rate of 50 mV/s.

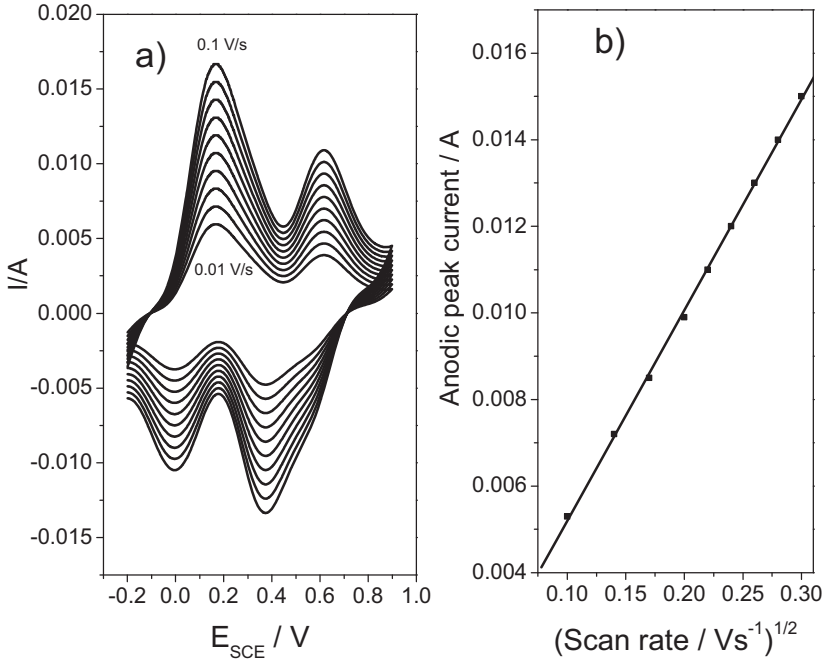

Fig. 4. (a) CVs of PANI 1 at different scan rates in 0.5 M H_2SO_4 (b) dependence of first anodic peak current on square root of scan rate.

This finding is also supported by UV–vis spectroscopy and XRD study as discussed in the following sections.

Generally, it is reported that in the presence of large molecules (surfactants as dopant), PANI shows low conductance [12,11]. In the present case HSO_4^- moieties are supposed to enhance electrical conductance of the material as the minimum resistance is 0.56 Ω for PANI 2 and 0.20 Ω for PANI 1. These values are indeed very good and are comparable with those of electrochemically synthesized polyaniline [26]. Hence, the polyaniline salts synthesized in the present study not only show very good solubility in most of the common organic solvents but also exhibit very good conductance in aqueous electrolytic media. Both of these properties are of high value for determining the importance of a material in various technologies.

3.5. UV–vis spectroscopy and in situ UV–vis spectroelectrochemistry

Fig. 6 shows the UV–vis spectra of PANI 1, PANI 2 and PANI 3. All samples show three characteristic absorption bands at 322–342 nm, 400–435 nm and 760–832 nm. The first band arises from π–π* transition within benzoid (B) ring of the polymer backbone, the second and third absorption bands are due to the polaron–π* (quinoid Q ring) and π–polaron transition (exciton), respectively [27]. The second and third peaks are related to the doping level and formation of polaron which support the formation of emeraldine salt form of PANI [28].

The appearance of the well defined band in the red region suggests the formation of PANI samples with good conjugation length. The weakened steric hindrance between dopant and PANI chain might be a cause of it [29]. The variation of peak intensity and wavelengths can be related to degree of doping, conjugation length of polyaniline chain and solubility of polyaniline in a solvent [29].

Detailed spectroelectrochemical investigations were carried out with thin PANI films dip coated onto the surface of an indium-doped tin oxide (ITO) coated glass electrode. Fig. 7 shows the absorption spectra of PANI 1 film on ITO glass electrode at stepwise increased electrode potentials from E_{SCE} = – 0.20 to 0.90 V. The main feature in the spectra are essentially the same as reported earlier [30] for electrochemically synthesized PANI, where three absorption peaks, which depend both in magnitude and position on potential, can be distinguished. The absorption around λ = 315 nm is caused by the π → π* electronic transition of benzoid rings and is characteristic of the leucoemeraldine form of PANI.

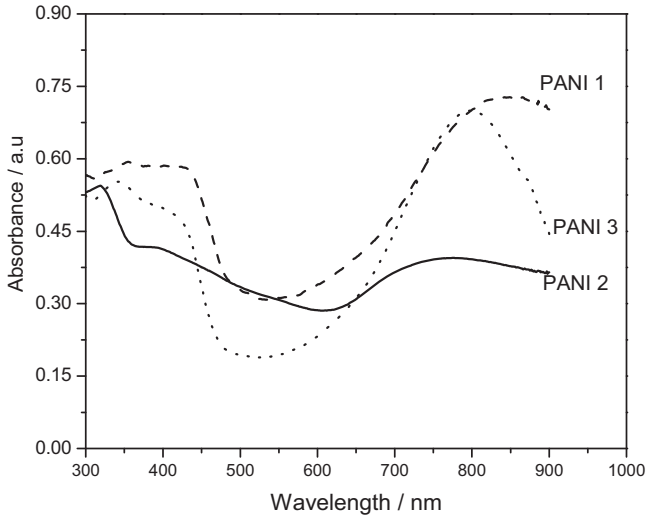

Fig. 6. UV–vis spectra of PANI-DBSA-HSO_4 salts recorded in ethanol (0.01 g/mL). The samples were synthesized using different amounts of H_2SO_4.

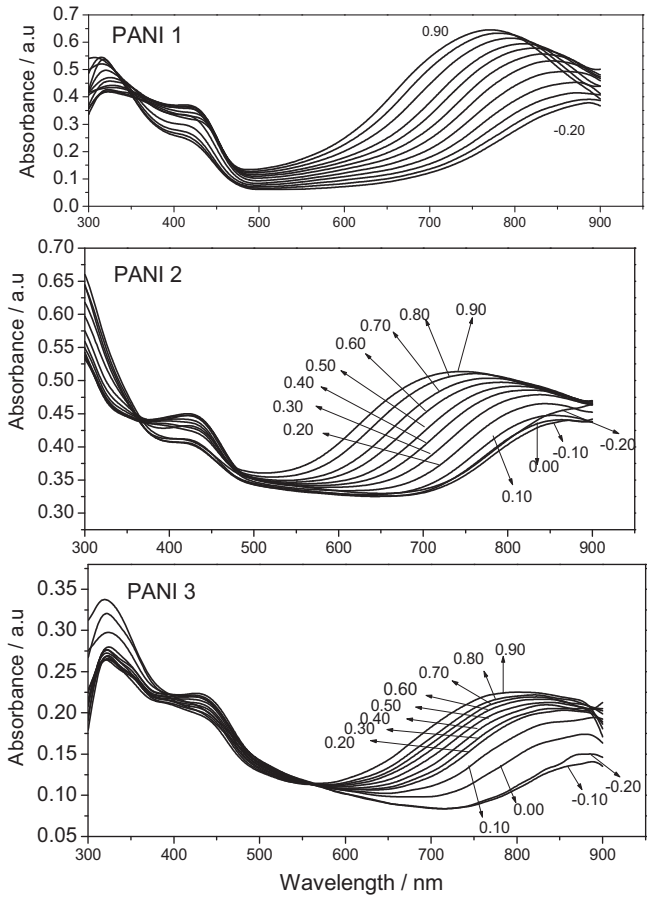

Fig. 7. In situ electronic absorption spectra of PANI 1, PANI 2 and PANI 3 recorded in anodic direction E_{SCE} = – 0.20 to 0.90 V.

The decrease in intensity of this band with increasing potential indicates diminished concentration of the reduced sites because of their transformation into oxidized sites. The absorbance band located at about λ = 420 nm also shows sensitivity to potential variations. It increases with potential up to E_{SCE} = 0.40 V and then decreases with further potential increase. This is close to the behavior of an intermediate species identified as radical cation or polaron formed during electrooxidation of the leucoemeraldine state of PANI [31]. The band most sensitive to the potential change is the low-energy polaron band. On one side the absorbance of this band increases continuously with the progressive increase of potential. On the other side it exhibits hipsochromic shift with the potential increase. This may be due to incorporation of more and more sulfate ions with increasing potential resulting in the formation of a compact coil structure [11]. The blue shift is more conspicuous at potentials above E_{SCE} = 0.70 V. This is usually attributed to the transformation of emeraldine into the completely oxidized pernigraniline state. This is confirmed by disappearance of the other polaron band at λ = 430 nm at potentials beyond E_{SCE} = 0.70 V. In case of PANI 2 and PANI 3 the absorbance of this band decreases by increasing the potential from E_{SCE} = – 0.20 to – 0.1 V. Beyond this potential the absorbance of this band increases with the potential increase. PANI exists in its leucoemeraldine form in the potential range of E_{SCE} = – 0.20 to – 0.1 V. The increase of absorbance at E_{SCE} = – 0.1 V might be indicative of the conversion of leucoemeraldine into the emeraldine salt form of PANI. Clearly, we observed an isosbestic point with PANI 2 at λ = 360 nm in between the bands at λ = 315 nm and 420 nm which is normally attributed to a one step transformation from emeraldine to pernigraniline [11]. With PANI 3 two isosbestic points were obtained: the first between

λ = 315 nm and 420 nm as with PANI 2 and the second at about λ = 570 nm between the bands at λ = 420 nm and 800 nm. Similar trends were also observed by Albuquerque et al. [32] which they assigned to the interconversion of three states of PANI i.e., leucoemeraldine, emeraldine and pernigraniline.

In order to check electrochromic reversibility of the polymer film, electronic absorption spectra were also recorded in cathodic direction (Fig. 8). The plots of absorbance and wavelength of low energy polaron band vs. applied potential are given in Fig. 9. These figures indicate that PANI films have very good electrochromic reversibility.

3.6. FT-IR spectroscopy

Fig. 10 represents FT-IR spectra of PANI salts and the corresponding bands along with their assignment are given in Table 2. PANI 1 and PANI 3 show almost the same spectral behavior whereas the bands for PANI 2 appear at lower wave numbers. The shift of the peaks observed with PANI 1 and PANI 3 illustrates a more intimate interaction between the polymers and dopant [33]. In case of PANI 1 and PANI 3 the main characteristic peaks observed at 1581 and 1505 cm^{-1} are attributed to quinoid and benzoid units respectively [34,35]. The band at 1310 cm^{-1} is attributed to C—N stretching of PANI backbone [34]. However, as discussed above, these characteristic bands for PANI 2, appearing at 1470 and 1580 cm^{-1}, are due to benzoid and quinoid stretching, respectively [36]. The band at 1303 cm^{-1} indicates C—N stretching vibration of the backbone of PANI [37].

Beside these peaks, some peaks are observed at the same position for all the samples: The peak at about 1140 cm^{-1} is due to the plane vibration of Q=NH^+—B and B—N^+H—B which is formed during protonation and is considered to be a measure of electron delocalization in PANI chain and thus a characteristic peak related to PANI conductance [38]. The peak at 1150 cm^{-1} is assigned to electronic or vibrational band of nitrogen quinone [39]. The bands at about 510 cm^{-1} observed in all spectra can be assigned to the absorption of the sulfonate anion of DBSA [40]. Furthermore, all the spectra clearly indicate that all PANI samples contained hydrogen sulfate counterions showing a band at 613 cm^{-1} [41]. All these well defined peaks confirmed that both DBSA and hydrogen sulfate moieties are properly incorporated in the PANI chain.

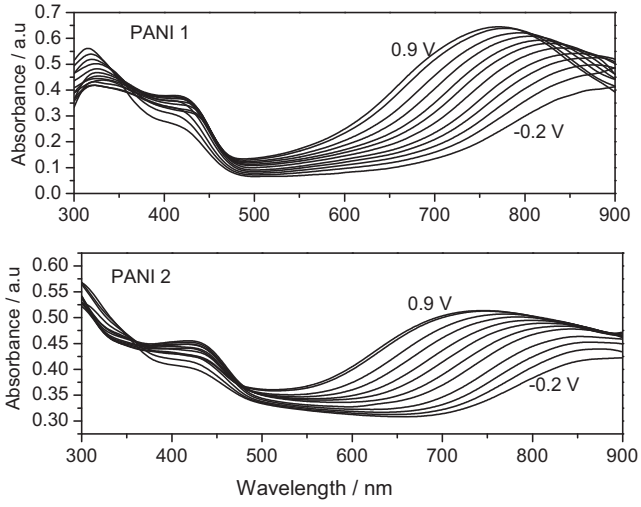

Fig. 8. In situ electronic absorption spectra of PANI–DBSA–H_2SO_4 salts recorded in cathodic direction E_{SCE} = 0.90 to − 0.20 V.

3.7. X-ray diffraction

Fig. 11 shows the influence of increasing acidity in the feed on the X-ray patterns of PANI–DBSA–H_2SO_4. All the patterns show a well-defined peak centered at $2\theta = 25^\circ$. This peak is assigned to the van der Waals distance between stacks of phenylene rings [42]. However, additional peaks at $2\theta = 19–36^\circ$ observed for PANI 1 indicate that the overall crystallinity of this sample is higher as compared to other samples [43]. Better crystallinity of PANI 1 can be attributed to its well organized and regular structure. Hence, the increase in crystallinity of PANI 1 is expected to increase its conductance [44]. This statement is supported by conductance measurements discussed earlier.

3.8. Thermogravimetric analysis

Thermal stability of a polymer is very important for its technological applications. The use of conducting polymers in industry is limited due to their undesirable properties such as loss of dopant and decomposition at high temperature. Moreover, due to the loss of conductance at high temperature, their use in electronic devices, solid sate batteries, chemical sensors, electromagnetic shielding, anticorrosion coatings etc, has been restricted [45]. In the present study thermal degradation of PANI was monitored through thermogravimetry. The results are presented in Fig. 12.

The polyaniline salts synthesized at room temperature showed three main weight loss stages [6]. The first weight loss at about 260 °C is associated with the loss of moisture. PANI always shows high moisture loss because it is highly hygroscopic in nature and some moisture still remains even after vacuum drying [44]. The second weight loss in the range 260–500 °C is attributed to degradation of the dopant. The slow and somewhat gradual weight loss which is observed at temperature higher than 500 °C is due to the structural decomposition of the PANI backbone [6]. All PANI samples did not destroy completely. A possible reason might be the fact that in nitrogen atmosphere carbonization of polymer takes place leaving a marked residue [6]. The results indicate that PANI–DBSA–H_2SO_4 synthesized in the present work is thermally more stable as compared to those reported in literature [46,47,48]. Generally, the surfactants exhibit a low thermal stability; however, in the present case the results indicate that the percentage of surfactant in the final conducting product is low enough. This does not affect the overall thermal stability of the product. These highly thermally stable polymers can be effectively used in various technological applications where working at an elevated temperature is required.

3.9. Intrinsic viscosity

The viscosity behavior of macromolecular substances in solution is one of the most frequently used approaches for characterization. Intrinsic viscosities of PANI–DBSA–H_2SO_4 salts (Table 3) show an appreciable change in the intrinsic viscosity of the polymers with increasing amount of the acid in the feed. However, with further increasing the amount of acid both yield and intrinsic viscosity decrease possibly due to high acidity-accelerated degradation of the PANI chain [18]. The intrinsic viscosity values in Table 3 illustrate that the polymers have highest intrinsic viscosity than any other intrinsic viscosity values reported for PANI, and hence indicate highest molecular weight of the materials as compared with the reported literature [17,18].

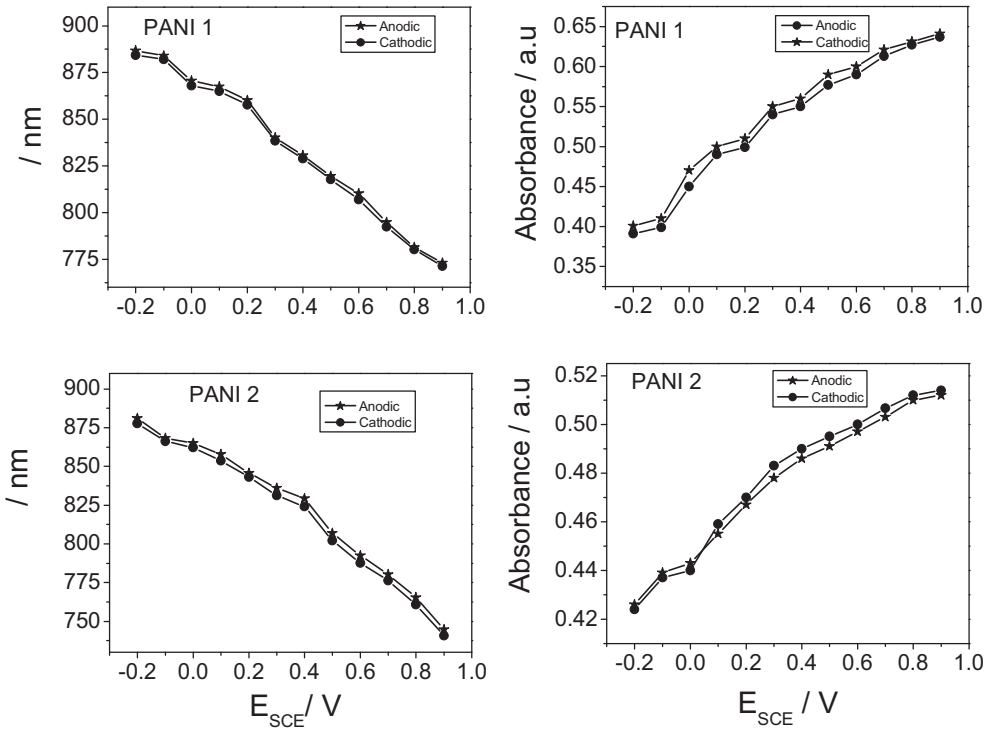

Fig. 9. Change in the position and absorbance of the low-energy polaron band with the applied potential (positive and negative direction).

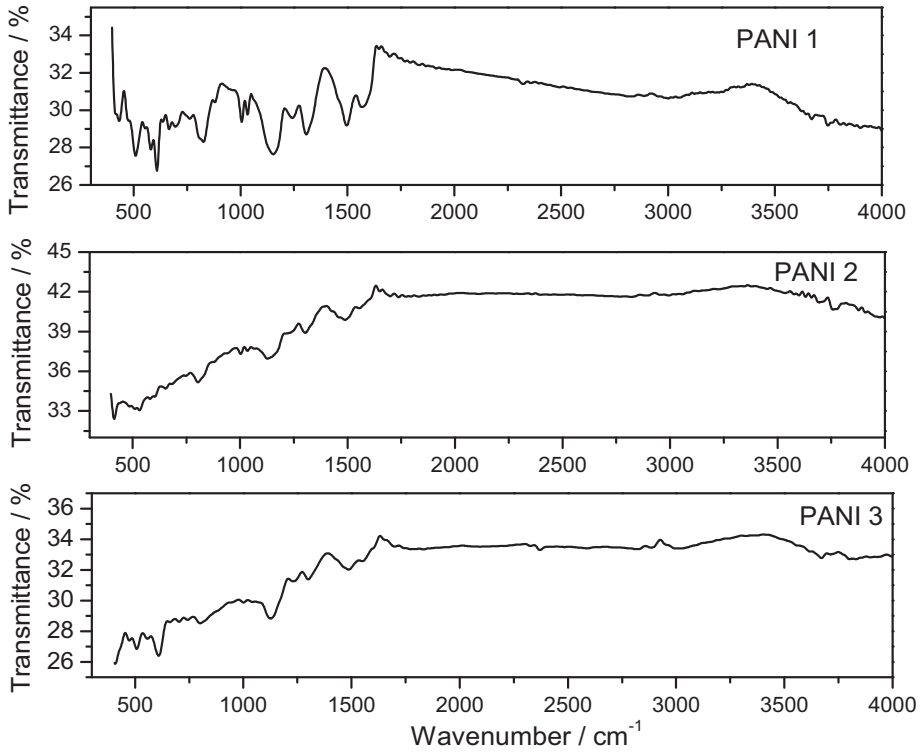

Fig. 10. FT-IR spectra of PANI 1, PANI 2 and PANI 3, as indicated.

3.10. Morphology of PANI–DBSA–H_2SO_4

Scanning electron micrographs of PANI–DBSA–H_2SO_4 synthesized with different amounts of the acid (Fig. 13) show granular morphology for PANI 1 and PANI 2. However, for PANI 3 the granular morphology changes to block shape which might be attributed to the change in micellar shape [27]. The morphology of PANI depends upon the method of synthesis and solvent or medium [49]. Shreepathi and Holze [11] studied the influence of the amount of DBSA in the feed on morphology of PANI in an inverse emulsion polymerization pathway. They found that PANI–DBSA exhibits fibrillar and porous network morphology. Han et al.

Table 2
Band assignments of FT-IR spectra of PANI–DBSA–H_2SO_4 salts. Assignments are based on Ref. [33–41].

Band position, Wave number (cm^{-1})			Band assignment
PANI 1	PANI 2	PANI 3	
1581	1581	1580	Quinoid stretching
1505	1505	1470	Benzoid stretching
1310	1310	1303	C—N stretching
1140	1140	1140	Vibration of Q=NH^+—B and B—N^+H—B
1150	1150	1150	Nitrogen quinone
510	510	510	Sulfonate anion of DBSA
613	613	613	Hydrogen sulfate

[27] reported one step reverse micelle polymerization of PANI–DBSA which showed spherical morphology. In the present study the granular morphology of the PANI–DBSA–H_2SO_4 can be due to the polymerization of aniline in the presence of strong acid (H_2SO_4) [50,51]. It is assumed that in strongly acidic medium the induction period of polymerization is short. Thus the available time is not sufficient for the organization of phenazine nucleates, consequently resulting in the granular morphology of PANI [52]. All the micrographs show very good porosity which is considered suitable for immobilization of bio-components and can be used in biosensors.

3.11. Corrosion protection performance of PANI–DBSA–H_2SO_4

As a matter of fact, for the very long time, corrosion of steel is a serious problem throughout the world. Corrosion of steel structures in the marine environment is a major problem than inland. Steel is recognized as the premium material for marine applications where it is used for its excellent corrosion resistance, luster, strength and stiffness. The applications include coastal handrails, housings for equipment, ladders, lamp posts, submerged items (pipelines and grills for oil, sewage and water), risers for oil platforms, grills, heat exchangers for ships and coastal power plants, equipment attached to hulls of boats and ships etc., The deterioration of these kinds of structures is very costly and dangerous for environment. Steel substrates are more prone to corrosion in a marine environment than inland due to galvanic cell formation and erosion of products.

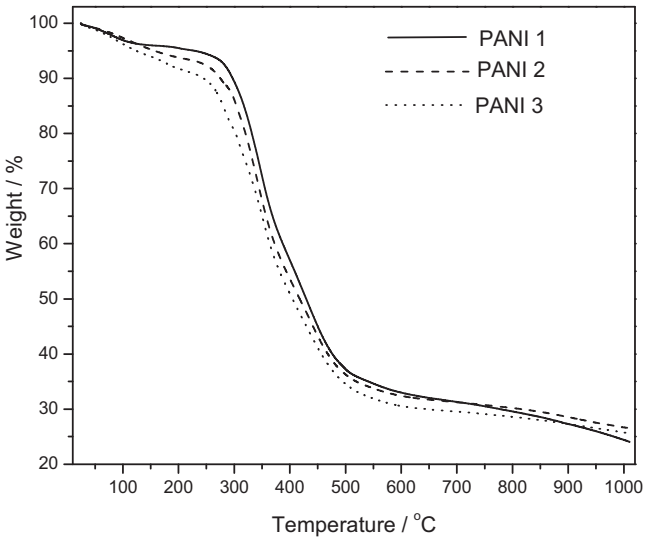

Fig. 12. Thermogravimetric curves recorded for PANI 1, PANI 2 and PANI 3, as indicated.

Various anti-corrosive pigments such as zinc phosphate, chromates and lead compounds can be used in paint systems to control corrosion [53]. However, these pigments should be eliminated from environment due to their severe toxicological properties [53]. Moreover, these corrosion inhibiting coatings onto steel object are not a complete solution because these coatings are subjected to scratches, cracks and chips which again expose the metal to the corrosive environment. Even very small pinhole size discontinuities in a coating can be problematic. It has been found that the effects of corrosion at discrete locations (due to chips and scratches) are harsher because the corrosive elements are concentrated at the point of exposure [54]. Accordingly,

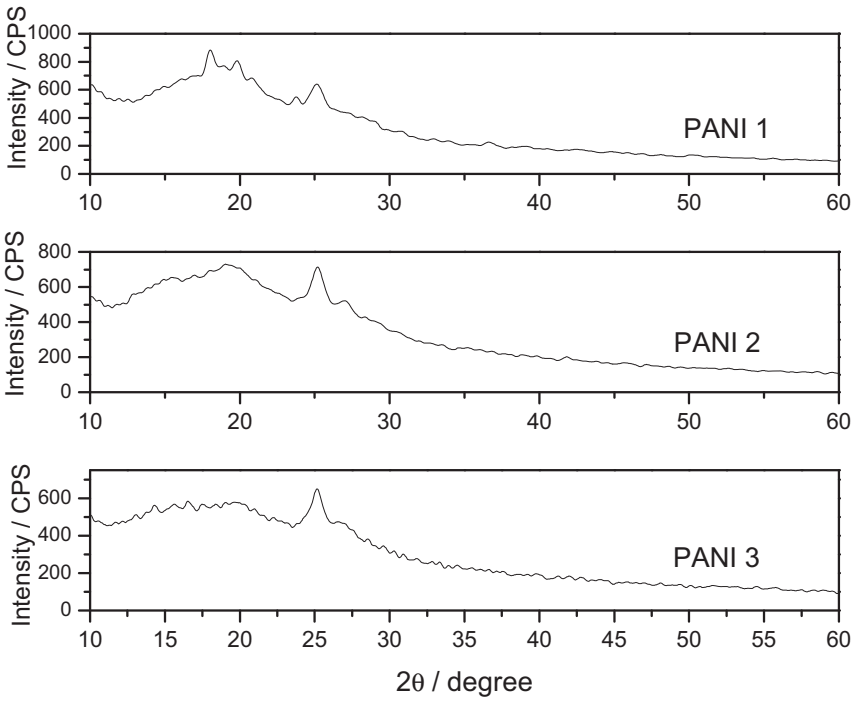

Fig. 11. X-ray diffraction patterns of PANI 1, PANI 2 and PANI 3, as indicated.

Table 3
Change of intrinsic viscosity with change in the acid concentration.

Sample	Intrinsic viscosity η/ mL/g
PANI 1	198
PANI 2	212
PANI 3	109

conventional corrosion inhibiting coatings are not satisfactory for corrosion protection of steel objects. Therefore, environment friendly and effective corrosion inhibitors are required.

Polyaniline salts exhibiting interesting redox properties offer good alternative. These materials are well adhesive and form a passive oxide layer showing tolerance for scratches and pin holes unless accidentally or intentionally made with a sharp tool. Several reports indicate a beneficial corrosion protection of steel alloys by PANI in different corrosion environments such as saline water [55], acids [56], concrete [57] and sand [58]. These studies suggested PANI as a potential corrosion inhibiting material. However, most of the studies have been carried out in the electrolyte solutions prepared in laboratory. To the best of our knowledge, there is no report on its practical applicability for marine/ocean environment which is a complex chemical system and more aggressive corrosive environment than the laboratory prepared electrolytes. It possesses salinity, various minor ions, complex biological activity and has access dissolved oxygen, and pollutants [59]. The PANI synthesized in the present work was tested for the corrosion protection of various grades of steel. For this purpose the experiments were performed in the natural water of Oceans. The coatings showed excellent corrosion protection efficiency for steel.

The representative Tafel plots of uncoated and PANI 1 coated steel electrodes in natural water of the Oceans are shown in Fig. 14. The corresponding values of E_{cor}, i_{cor}, CR and protection efficiency are summarized in Tables 4 and 5. The PANI 1 coated electrodes showed a remarkable potential shift and reduction i_{cor} and CR values as compared to uncoated steels. The positive shift of corrosion potential and reduction in the i_{cor} of the coated steel implies that these polymer coatings can provide a best protection to stainless and mild steel against corrosion in the waters of ocean. The better performance might be attributed to the high solubility, good electrical conductance and redox reversibility of the synthesized PANI salts.

Tables 4 and 5 show some differences in the values of all parameters (E_{cor}, i_{cor} and CR) calculated for two kinds of PANI 1 coated steels in two different kinds of water (water from Indian and Pacific Oceans). In the water of the Indian Ocean the E_{cor} shift after coating is small (E_{SCE} = 0.15 V) for stainless steel, and it is large (E_{SCE} = 0.4 V) for mild steel. In case of water of the Pacific Ocean the E_{cor} shift for the stainless steel is also small (E_{SCE} = 0.19 V) and for the mild steel it is large (E_{SCE} = 0.2 V).

Likewise, the value of i_{cor} show a strong decrease both for coated stainless steel and mild steel in water of the Indian Ocean. While for water of the Pacific Ocean the difference in the values of i_{cor} of uncoated and coated steels is not so high.

Similarly, variations can be observed in the values of corrosion rate (CR) calculated for all these systems. The CR greatly decreases by a factor of 16.6 mm/year for coated stainless steel as compared to uncoated stainless steel, whereas it shows a shift of 23.2 mm/year for coated mild steel in water of the Indian Ocean. In the water of the Pacific Ocean a shift of 14.85 mm/year in CR can be observed for coated stainless steel and 15.52 mm/year for mild steel.

The pronounced shift in the values of above mentioned parameters and different behaviors of steels in the waters of Indian and Pacific Oceans can be explained on the basis of various factors. Generally, in a particular experiment, the values of E_{cor} shift, i_{cor} and CR can be expected to affect by the nature of coating, type of substrate, and type and concentration of the electrolyte used. It is an established fact that, when used as a coating on a substrate, the adequate oxidizing power of PANI allow it to readily form passivating iron oxide layer on the steel surface. This mechanism can be explained with the help of the following equations:

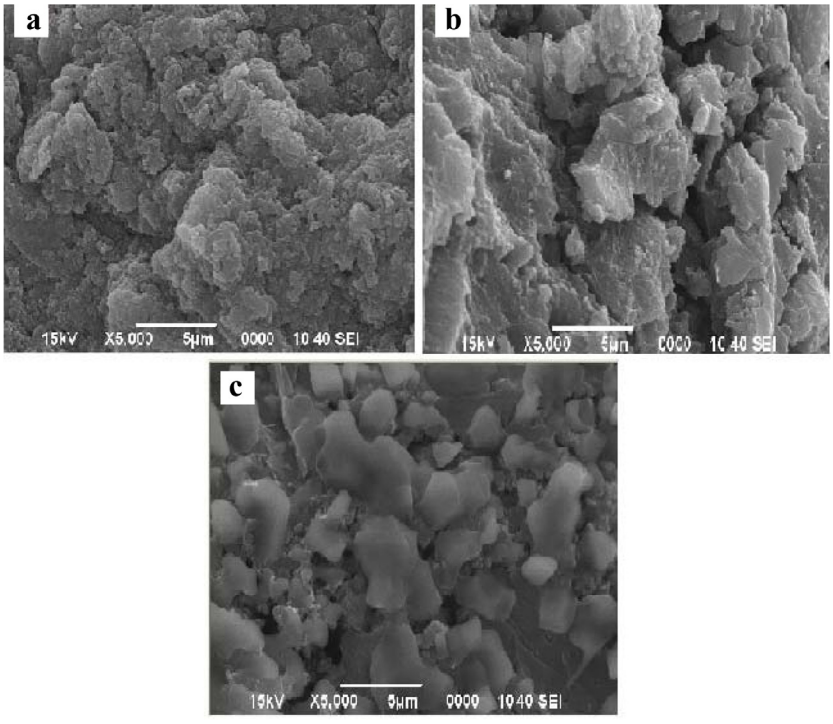

Fig. 13. Scanning electron micrographs of (a) PANI 1 (b) PANI 2 and (c) PANI 3.

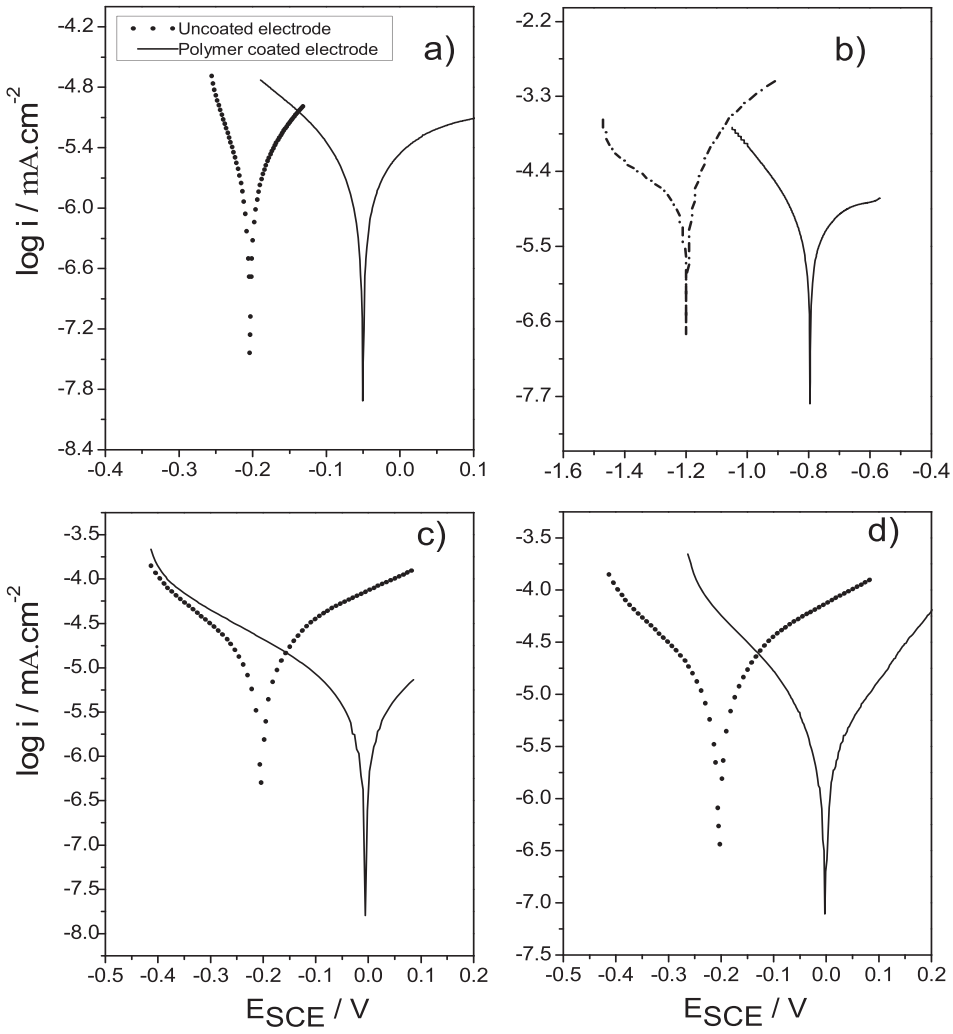

Fig. 14. Tafel plots recorded for PANI 1 coated (a) stainless steel and (b) mild steel electrode in the water of Indian Ocean and (c) stainless steel and (d) mild steel electrodes in water of Pacific Ocean.

Table 4
E_{cor},i_{cor} and CR values calculated from the Tafel plots recorded for PANI 1 coated steel electrodes in the water of Indian Ocean.

Parameter	Uncoated stainless steel	Coated stainless steel	Uncoated mild steel	Coated mild steel
E_{cor} (V)	−0.201	−0.051	−1.201	−0.799
i_{cor} (μA/cm^2)	38.70	2.26	19.64	5.10
CR (mm/year)	17.68	1.03	30.13	6.89

Table 5
E_{cor}, i_{cor} and CR values calculated from the Tafel plots recorded for PANI 1 coated steel electrodes in the water of Pacific Ocean.

Parameter	Uncoated stainless steel	Coated stainless steel	Uncoated mild steel	Coated mild steel
E_{cor} (V)	−0.206	−0.012	−0.205	−0.004
i_{cor} (μA/cm^2)	26.50	3.43	22.20	5.73
CR (mm/year)	15.95	1.10	18.14	2.62

(a)4 $2Fe\ (s) \rightarrow 2Fe^{2+} + 4e$

(b)5 $2Fe^{2+} \rightarrow 2Fe^{3+} + 2e$

(c)$ES + 4e \rightarrow LE$

(d)$0.5O_2 + H_2O + 2e \rightarrow 2OH^-$

(e)6 $2Fe^{3+} + 6OH^- \rightarrow Fe_2O_3 + 3H_2O$

(f)$LE + 2H_2O + O_2 \rightarrow ES + 4OH^-$

The above equations demonstrate that iron (Fe) can readily be oxidized to Fe^{2+} (Eq. (a)) and subsequently to Fe^{+3} (Eq. (b)). During this process PANI, in the emeraldine salt (ES) form, merely reduces to its leucoemeraldine (LE) form by accepting the electrons generated during the oxidation of iron (Eq. (c)) [60]. Meanwhile, these electrons can also combine with the dissolved oxygen in the aqueous medium to form OH^- ions (Eq. (d)). These OH^- ions further react with Fe^{+3} ions to form Fe_2O_3 (Eq. (e)). Thus the resultant Fe_2O_3 layer serves as a passivating layer on the steel surface. Additionally, the dissolved oxygen in the aqueous medium re-oxidizes LE back to ES (Eq. (f)) to regenerate the electron accepting ability of PANI [1]. This last oxidation step manifests that in the passivating process, PANI acts in the catalytic fashion. And so PANI with good electrochemical activity can provide good protection. However, in the present case the observed differences in values in Tables 4 and 5 can not be explicitly related with difference in the corrosion protection behavior of PANI as the same sample of PANI (i.e., PANI 1) was used in all the systems.

The second parameter that can be taken in consideration to be responsible for the differences in the values in Tables 4 and 5 is the nature of steel as a substrate. In this study, two types of steels (stainless steel and mild steel) were employed as a substrate. The difference in the values of corrosion parameters for the two types of steels can be related to their different metallography. It is a matter of fact that a protective coating on the steel substrate can acts as a physical barrier to the diffusion of corrosive media across it, and thus prevents corrosion of the underlying substrate. Thus, the firm adhesion of a coating at the steel surface is a crucial factor. The weak adherence of the coating on steel surface may allow the corrosive medium to access the surface of the steel substrate and breakdown its passivation. This process produces corrosion products that further affect the adherence of the coating onto the steel substrate. This type of miscarriage cannot be recovered by the dissolved oxygen in electrolyte (or possible redox property of PANI, if used as a coating) [61]. We observed during our experiments that PANI 1 coating on mild steel surface gives much adherent film than its coating on stainless steel surface. Therefore, the corrosion protection performance the PANI 1 was better for mild steel in comparison with its corrosion protection performance for stainless steel in the waters of both of the Oceans.

It can also be observed that the same sample of PANI (PANI 1) offer different corrosion protection to mild and stainless steel in the water of Indian and Pacific Ocean. This can be attributed to the difference in the composition of the waters of Indian and Pacific Oceans. Although in oceanography, salinity (concentration of dissolved salts) is a fundamental property of the water of an Ocean [62], yet it is not uniform even in the same ocean. The content of different ions may be different at different places. In general terms, these ions of the dissolved salts play an important role in corrosion protection by covering the steel surface with insoluble products and enhance passivation of the surface [60,63].

7. Conclusions

Processable PANI–DBSA–H_2SO_4 salts with high solubility and electrical conductance were successfully prepared by emulsion polymerization of aniline in the presence of DBSA and H_2SO_4. In addition, these salts were thermally stable up to 500 °C. The yield of the polymer was found to be strongly dependent on the polymerization conditions such as amounts of acid, oxidant and monomer. Cyclic voltammetry confirmed the good electroactivity and purity of the synthesized PANI salts. FTIR, UV–vis spectroscopy and X-ray diffraction results support the formation of PANI salts doped with DBSA and H_2SO_4. In conclusion, we have developed a novel and simple approach for the chemical oxidative polymerization of aniline based on the use of two dopants (DBSA and sulfuric acid) together for the synthesis of highly soluble, conducting and thermally stable PANI salts. These salts can effectively be used in various technologies where these qualities are required. Polarization measurements revealed that coatings of these PANI salts can provide excellent resistance to various grades of steel surfaces against harsh corrosive environment of the oceans.

Acknowledgments

Financial support from Higher Education Commission Islamabad, Pakistan (under the project # 20-1647), is gratefully acknowledged. Fonds der Chemischen Industrie, the Deutsche Forschungsgemeinschaft and a travel grant of Technische Universität Chemnitz to S.Bilal and A.A. Shah are gratefully acknowledged. Ms. Sadaf Tasneem and Mr. Mujahid Shah are gratefully acknowledged for providing water samples from Pacific and Indian Oceans. Support provided by Dr. Khalida Akhtar for recording scanning electron micrographs is greatly appreciated.

References

[1] R. Ansari, M.B. Keivani, Polyaniline conducting electroactive polymers: thermal and environmental stability studies, E-J. Chem. 3 (2006) 202.
[2] S. Bhadraa, D. Khastgir, N.K. Singhaa, J.H. Leeb, Progress in preparation, processing and applications of polyaniline, Prog. Polym. Sci. 34 (2009) 783.
[3] R.F. Bay, S.P. Armes, C.J. Pickett, K.S. Ryder, Poly(1-vinylimidazole-*co*-4-aminostyrene): steric stabilizer for polyaniline colloids, Polymer 32 (1991) 2456.
[4] S. Palaniappan, A. John, Polyaniline materials by emulsion polymerization pathway, Prog. Polym. Sci. 33 (2008) 732.
[5] M.E. Barra, M.M. Leyva, B.G. Gorelova, X-ray photoelectron spectroscopy and electrical conductivity of polyaniline doped with dodecylbenzenesulfonic acid as a function of the synthetic method, J. Appl. Polym. Sci. 80 (2001) 556.
[6] S. Bilal, S. Gul, K.A.A. Ali. Shah, Synthesis and characterization of completely soluble and highly thermally stable PANI–DBSA salts, Synth. Met. 162 (2012) 2259.
[7] G.I. Titelman, A. Siegmann, M. Narkis, Y. Wei, Morphology of polyaniline redoped by kneading with dodecylbenzene sulfonic acid, J. Appl. Polym. Sci. 69 (1998) 2205.
[8] Y. Cao, P. Smith, A.J. Heeger, Counter-ion induced processibility of conducting polyaniline and of conducting polyblends of polyaniline in bulk polymers, Synth. Met. 48 (1992) 91.
[9] C. Yu, J. Zhai, X. Gao, M. Wan, L. Jiang, T. Li, Z. Li, Water-assisted fabrication of polyaniline honeycomb structure film, J. Phys. Chem. B 108 (2004) 4586.
[10] M.G. Han, S.K. Cho, S.G. Oh, S.S. Im, Preparation and characterization of polyaniline nanoparticles synthesized from DBSA micellar solution, Synth. Met. 126 (2002) 53.
[11] S. Shreepathi, R. Holze, Spectroelectrochemical investigations of soluble polyaniline synthesized via new inverse emulsion pathway, Chem. Mater. 17 (2005) 4078.
[12] W. Yin, E. Ruckenstein, Soluble polyaniline co-doped with dodecyl benzene sulfonic acid and hydrochloric acid, Synth. Met. 108 (2000) 39.
[13] J. Stejskal, D. Hlavata, P. Holler, M. Trchova, J. Prokes, I. Sapurina, Polyaniline prepared in the presence of various acids: a conductivity study, Polym. Int. 53 (2004) 294.
[14] D.D. Borole, U.R. Kapadi, P.P. Kumbhar, D.G. Hundiwale, Effect of inorganic dopants (in presence of electrolyte) on the conductivity of polyaniline, poly(*o*-toluidine) and their copolymer thin films, Meter. Lett. 57 (2002) 844.
[15] P.S. Rao, D.N. Sathyanarayana, S. Palaniappan, Polymerization of aniline in an organic peroxide system by the inverted emulsion process, Macromolecules 35 (2002) 4988.
[16] R. Holze, J. Lippe, A method for electrochemical in situ conductivity measurements of electrochemically synthesized intrinsically conducting polymers, Synth. Met. 38 (1990) 99.
[17] J. Yang, B. Weng, Inverse emulsion polymerization for high molecular weight and electrically conducting polyanilines, Synth. Met. 159 (2009) 2249.
[18] A. Dan, P.K. Sengupta, Synthesis and characterization of polyaniline prepared in formic acid medium, J. Appl. Polym. Sci. 91 (2004) 991.
[19] P. Ghosh, S.K. Siddhanta, S.R. Haque, A. Chakrabart, Stable polyaniline dispersions prepared in nonaqueous medium: synthesis and characterization, Sythn. Met. 123 (2001) 83.
[20] M.M. Ayad, M.A. Sheneshin, Effect of acids on in situ polyaniline film formation, Polym. Int. 53 (2004) 1180.
[21] M.S. Ram, S. Palaniappan, A process for the preparation of polyaniline salt doped with acid and surfactant groups using benzoyl peroxide, J. Mater. Sci. 39 (2004) 3069.

[22] Y. Cao, J. Qui, P. Smith, Effect of solvents and co-solvents on the processibility of polyaniline: I. solubility and conductivity studies, Synth. Met. 69 (1995) 187–190.
[23] S. Palaniappan, C.A. Amarnath, A novel polyaniline–maleicacid–dodecylhydrogensulfate salt: soluble polyaniline powder, React. Funct. Polym. 66 (2006) 1741.
[24] S. Bilal, R. Holze, Electrochemical copolymerization of *o*-toluidine and *o*-phenylenediamine, J. Electroanal. Chem. 592 (2006) 1.
[25] G.D. Aprano, M. Leclerc, G. Zotti, Stabilization and characterization of pernigraniline salt: the acid-doped form of fully oxidized polyanilines, Macromolecules 25 (1992) 2145.
[26] A.A. Shah, R. Holze, Copolymers and two-layered composites of poly(*o*-aminophenol) and polyaniline, J. Solid State Electrochem. 11 (2006) 38.
[27] Y.G. Han, T. Kusunose, T. Sekino, One-step reverse micelle polymerization of organic dispersible polyaniline nanoparticles, Synth. Met. 159 (2009) 123.
[28] J. Yang, Y. Ding, G. Chen, C. Li, Synthesis of conducting polyaniline using novel anionic gemini surfactant as micellar stabilizer, Eur. Polym. J. 43 (2007) 3337.
[29] J. Kim, S. Kwon, D. Ihm, Synthesis and characterization of organic soluble polyaniline prepared by one-step emulsion polymerization, Curr. Appl. Phys. 7 (2007) 205.
[30] A.A. Shah, R. Holze, In situ UV–vis spectroelectrochemical studies of the copolymerization of *o*-aminophenol and aniline, Synth. Met. 156 (2006) 566.
[31] A. Malinauskas, R. Holze, Cyclic UV–vis spectrovoltammetry of polyaniline, Synth. Met. 97 (1998) 31.
[32] J.E. de Albuquerque, L.H.C. Mattoso, R.M. Faria, J.G. Masters, A.G. MacDiarmid, Study of the interconversion of polyaniline oxidation states by optical absorption spectroscopy, Synth. Met. 146 (2004) 1.
[33] J. Stejskal, M. Omastova, S. Fedorovac, J. Prokes, M. Trchova, Polyaniline and polypyrrole prepared in the presence of surfactants: a comparative conductivity study, Polymer 44 (2003) 1353.
[34] J.Y. Kwon, E.Y. Kim, H.D. Kim, preparation and properties of waterborne-polyurethane coating materials containing conductive polyaniline, Macromol. Res. 12 (2004) 303.
[35] S. Palaniappan, P. Maniskar, Electropolymerisation and characterisation of nanosize conducting poly[(*o*-chloroaniline)-*co*-(4,4′-diaminodiphenylsulfone)] on a polyaniline-modified electrode, Polym. Int. 59 (2010) 456.
[36] M.D. Kondawar, Transport properties of conductive polyaniline nanocomposites based on carbon nanotubes, Int. J. Compos. Mater. 2 (2012) 32.
[37] M.R. Nabid, Z. Zamiraei, R. Sedghi, N. Safari, Cationic metalloporphyrins for synthesis of conducting, water-soluble polyaniline, React. Funct. Polym. 69 (2009) 319.
[38] P. Liu, Synthesis and characterization of organo-soluble conducting polyaniline doped with oleic acid, Synth. Met. 159 (2009) 148.
[39] S. Palaniappan, C.A. Amaranth, Polyaniline-dodecylhydrogensulfate-acid salt: synthesis and characterization, Mat. Chem. Phys. 92 (2005) 82.
[40] J. Yang, Y. Ding, J. Zhang, Uniform rice-like nanostructured polyanilines with highly crystallinity prepared in dodecylbenzene sulfonic acid micelles, Mater. Chem. Phys. 112 (2008) 322.
[41] N.V. Blinova, J. Stejskal, M. Trchova, J. Prokes, Polyaniline prepared in solutions of phosphoric acid: Powders, thin films, and colloidal dispersions, Polymer 47 (2006) 42.
[42] C. Saravanan, S. Palaniappan, F. Chandezon, Synthesis of nanoporous conducting polyaniline using ternary surfactant, Mater. Lett. 62 (2008) 882.
[43] A.A. Athawale, M.V. Kalkarni, V.V. Chabukswar, Studies on chemically synthesized soluble acrylic acid doped polyaniline, Mat. Chem. Phys. 73 (2002) 106.
[44] S. Bhadra, S. Chattopadhyay, N.K. Singha, D. Khastgir, Improvement of conductivity of electrochemically synthesized polyaniline, J. Appl. Polym. Sci. 108 (2008) 57.
[45] T. Chen, C. Dong, X. Li, J. Gao, Thermal degradation mechanism of dodecylbenzene sulfonic acid-hydrochloric acid co-doped polyaniline, Polym. Degrad. Stab. 94 (2009) 1788.
[46] V.B. Chanshetty, S. Kalyane, S. Godiganur, Surface morphology studies and thermal analysis of V_2O_5 doped polyaniline composites, Int. J. Eng. Res. Appl. 2 (2012) 611.
[47] M. Jayakannan, P. Anilkumar, A. Sanju, Synthesis and characterization of new azobenzenesulfonic acids doped conducting polyaniline, Eur. Polym. J. 42 (2006) 2623.
[48] N.K. Svelko, S.J. Reynaud. Francois, Synthesis and characterization of polyaniline prepared in the presence of nonionic surfactants in an aqueous dispersion, Synth. Met. 150 (2005) 107.
[49] S. Sinha, S. Bhadra, D. Khastgir, Effect of dopant type on the properties of polyaniline, J. Appl. Polym. Sci. 112 (2009) 3135.
[50] J. Stejskal, I. Sapurina, M. Trchova, E.N. Konyushenko, Oxidation of aniline: polyaniline granules Nanotubes, and oligoaniline microspheres, Macromolecules 41 (2008) 3530.
[51] E.N. Konyushenko, J. Stejskal, I. Sedenova, M. Trchova, I. Sapurina, M. Cieslar, J. Prokes, Polyaniline nanotubes: conditions of formation, Polym. Int. 55 (2006) 31.
[52] I. Sapurina, J. Stejskal, The mechanism of the oxidative polymerization of aniline and the formation of supermolecular polyaniline structure, Polym. Int. 57 (2008) 1295.
[53] A. Sakhri, F.X. Perrin, E. Aragon, S. Lamouric, A. Benaboura, Chlorinated rubber paints for corrosion prevention of mild steel: A comparison between zinc phosphate and polyaniline pigments, Corros. Sci. 52 (2010) 901.
[54] P.J. Kinlen, D.C., Silverman, E.F., Tokas, C.J. Hardiman, Corrosion inhibiting compositions, U. S. Patent 5,532,025, 1996.
[55] V. Rajasekharan, T. Stalin, S. Viswanathan, P. Manisankar, Electrochemical evaluation of anticorrosive performance of organic acid doped polyaniline based coatings, Int. J. Electrochem. Sci. 8 (2013) 11327.
[56] S. Sathiyanarayanan, S. Muthukrishnan, G. Venkatachari, D.C. Trivedi, Corrosion protection of steel by polyaniline (PANI) pigmented paint coating, Prog. Org. Coat. 53 (2005) 297.
[57] K. Saravanan, S. Sathiyanarayanan, S. Muralidharan, S.S. Azim, G. Venkatachari, Performance evaluation of polyaniline pigmented epoxy coating for corrosion protection of steel in concrete environment, Prog. Org. Coat. 59 (2007) 160.
[58] A.R. Elkais, M.M. Gvozdenovic, B.Z. Jugovic, B.N. Grgura, The influence of thin benzoate-doped polyaniline coatings on corrosion protection of mild steel in different environments, Prog. Org. Coat. 76 (2013) 670–676.
[59] H. Moller, P.C. Pistorius, The influence of Sr^{2+} on the formation of calcareous deposits on freely corroding low carbon steel in seawater, J. S. Afr. Inst. Min. Metall. 107 (2006) 168.
[60] N. Ahmad, A.G. MacDiarmid, Inhibition of corrosion of steels with the exploitation of conducting polymers, Synth. Met. 78 (1996) 103–110.
[61] J. Fang, K. Xu, L. Zhu, Z. Zhou, H. Tang, A study on mechanism of corrosion protection of polyaniline coating and its failure, Corros. Sci. 49 (2007) 4232–4242.
[62] M.P.M. Reddy, Descriptive Physical Oceanography, Swets and zeitlinger, India, 2001.
[63] A.H.E. Shazly, H.A.A. Turaif, Improving the corrosion resistance of buried steel by using polyaniline coating, Int. J. Electrochem. Sci. 7 (2012) 211.